Supporting Information

Ethylene Glycol Emissions from On-road Vehicles

Ezra C. Wood[1], W. Berk Knighton[2], Ed C. Fortner[3], Scott C. Herndon[3], Timothy B. Onasch[3], Jonathan P. Franklin[3], Doug R. Worsnop[3], Timothy R. Dallmann[4], Drew R. Gentner[4], Allen H. Goldstein[4,5], Robert A. Harley[4]

[1] Department of Chemistry, University of Massachusetts, Amherst MA

[2] Department of Chemistry and Biochemistry, Montana State University, Bozeman MT

[3] Aerodyne Research, Inc., Billerica MA

[4] Department of Civil and Environmental Engineering, University of California, Berkeley CA

[5] Department of Environmental Science, Policy and Management, University of California, Berkeley CA

The SI contains 14 pages of additional information, including 6 figures.

1. Sampling Ethylene Glycol at the Caldecott Tunnel

Adsorption of EG onto the 34 m sampling tube and the internal surfaces of the PTR-MS was evident by the time response of the m/z 45 signal during dry zero air overblows and when the PTR-MS switched to sampling from its catalyst. When m/z 45 mixing ratios were high (over 20 ppb), the 1/e time response in the m/z 45 signal exceeded one minute when the PTR-MS was switched over to the catalyst (102 sec ± 5 sec on 27 July 2010, Figure SI-S1), compared to ~2 seconds for other VOCs measured. Similarly, m/z 45 levels rapidly decreased during zero air overblows but remained elevated (figure SI-2).

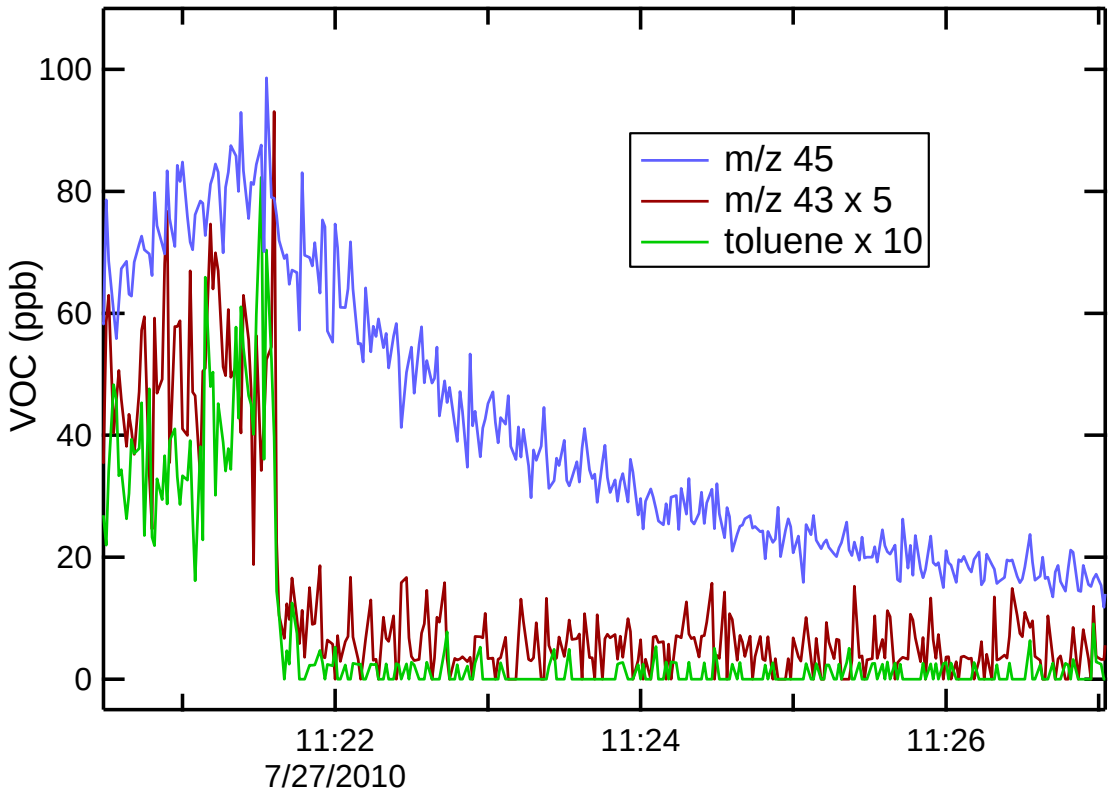

Figure SI-S1.

Time response of the PTR-MS when switched to catalyst sampling (at 11:21:30) after sampling high concentrations (80 ppb) of ethylene glycol. The much longer time response of m/z 45 (1/e

decay time of 102 ± 5 s) vs. toluene and m/z 43 (mostly propene) indicate adsorption and desorption of EG from the internal surfaces of the PTR-MS.

A.

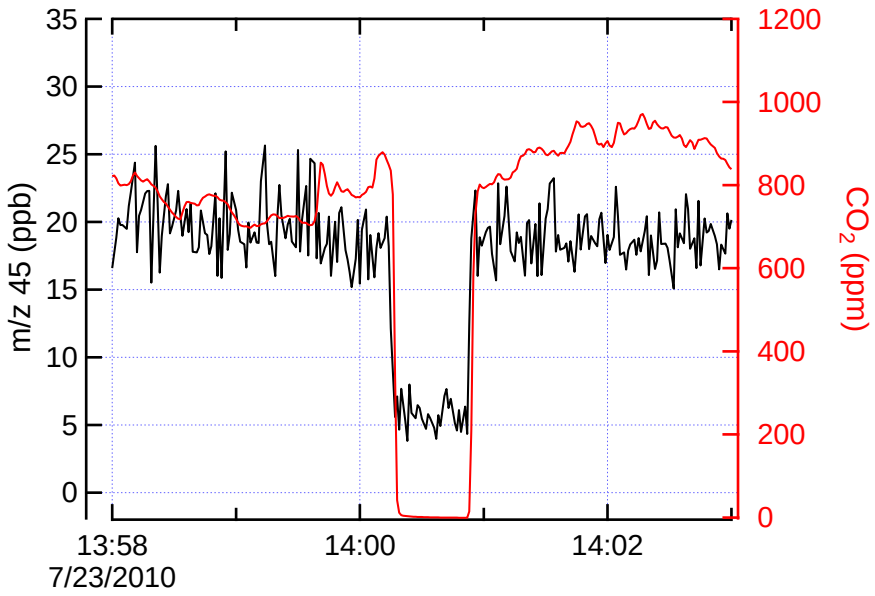

B.

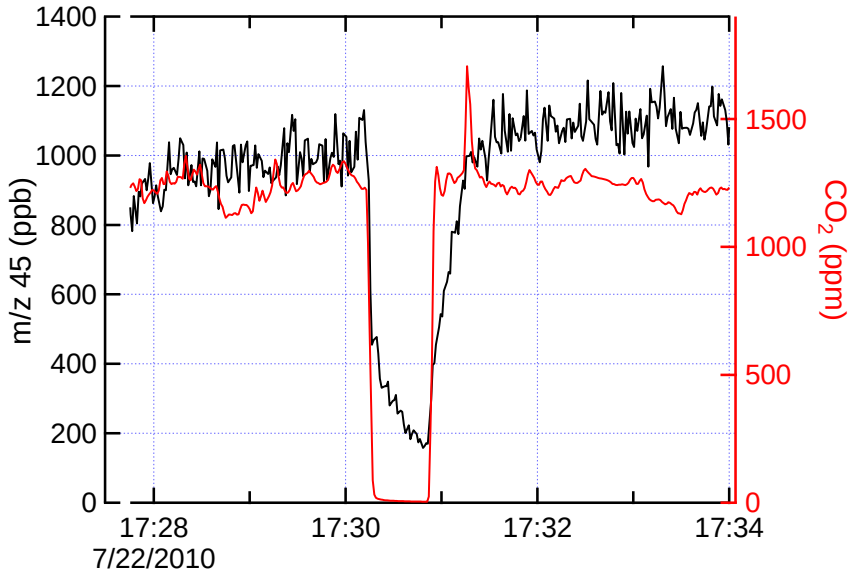

Figure SI-S2.

A. Zero air overblow data when sampling 20 ppb m/z 45 (mostly EG, not acetaldehyde). Desorption of EG from the tubing and PTR-MS led to the persistent ~6 ppb value during the overblow.

B. Zero air overblow when sampling 1000 ppb m/z 45. After a minute of sampling zero air, the PTR-MS still reads over 200 ppb of m/z 45. Reversible uptake and desorption of EG onto the sampling system is evident from the equal time response at the beginning and end of the zero air overblow.

2. Outdoor measurements of m/z 45 using the 34 m sampling tube

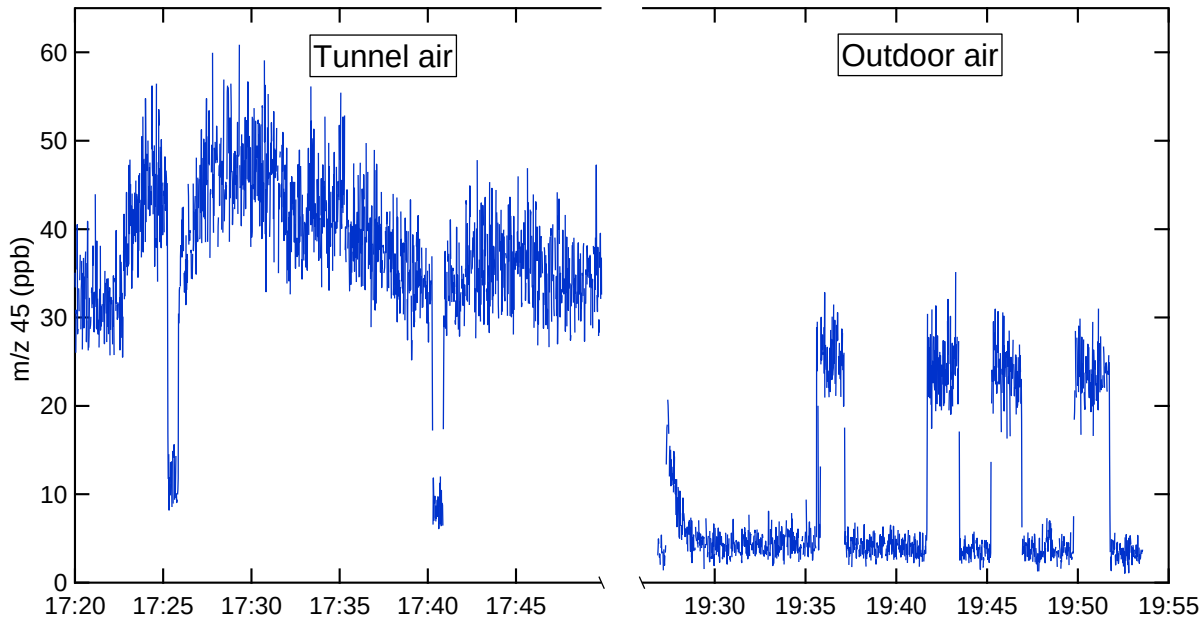

Figure SI-S3

Measurements of tunnel air and outdoor air on 27 July 2010. The PTR-MS sampled tunnel air from 17:20 to 17:50 (zero air overblows at 17:25 and 17:40). The high (30+ ppb) mz 45 mixing ratios are mostly from EG. From 19:25 to 19:55, the PTR-MS sampled outdoor air using the same filter and long sampling tube. The m/z 45 value of 4 ppb is reasonable for outdoor acetaldehyde (with a minor contribution from EG) and indicates that the high m/z 45 values observed while sampling from the tunnel were not from long-term inlet contamination. The periodic readings of ~25 ppbv starting at 19:35 are from standard additions of acetaldehyde. Outdoor EG concentrations are much lower than the tunnel because of the much higher dilution rates. The differences between tunnel and outdoor acetaldehyde concentrations (4 ppb outdoors at 19:30 on 7/27/2010 compared to tunnel concentrations of 2 to 13 ppb) are not as great because background atmospheric acetaldehyde accounts for a large portion of the acetaldehyde measured inside the tunnel.

4. Nighttime measurements of m/z 45 (PTR-MS) and CH_3CHO (GC) at the Caldecott Tunnel

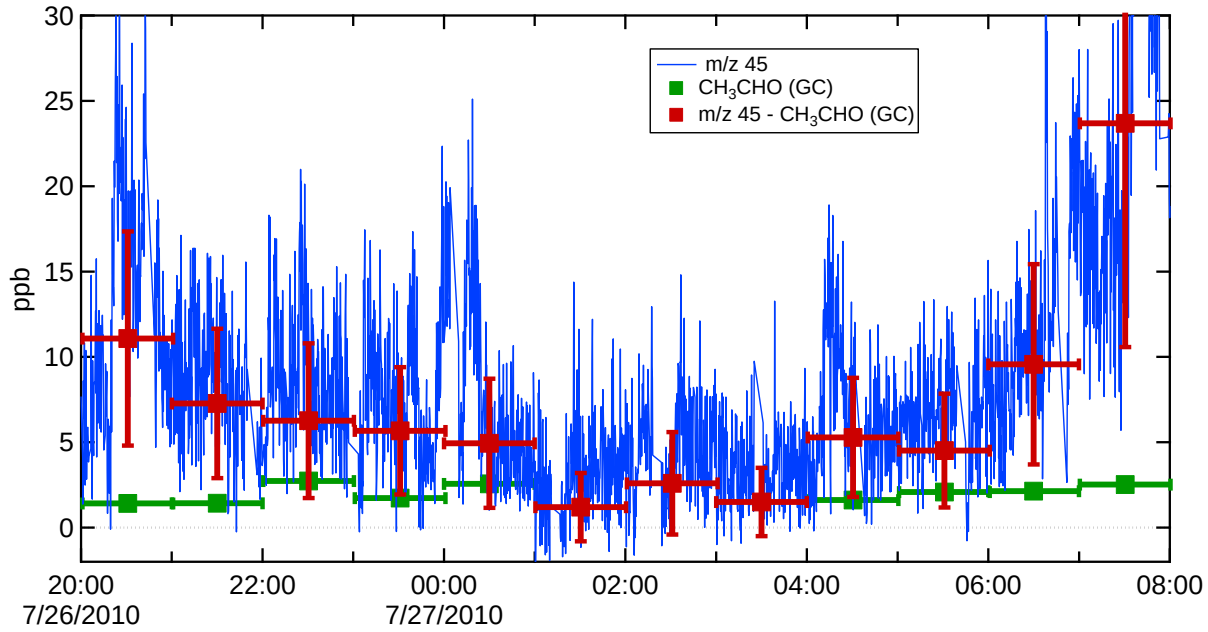

Figure SI-S4.

Mixing ratios of m/z 45 (PTR-MS, 14 s data), CH_3CHO (GC-FID, 1 hr data), and EG (calculated by difference) in the Caldecott Tunnel the night of 26 July 2010. The midpoint of the 1-hr average CH_3CHO and calculated EG mixing ratios are shown as squares. The 60-minute averaged EG mixing ratio was calculated by the difference between the m/z 45 (PTR-MS) and CH_3CHO (GC) mixing ratios. An estimated CH_3CHO mixing ratio of 2 ppb was used between 01:00 and 04:00 when the GC was off-line. The calculated EG concentrations are low and between 01:00 and 04:00 smaller than the measurement uncertainty.

5. Estimate of the ventilation rate in the Caldecott Tunnel.

We estimate the ventilation rate in the Caldecott Tunnel using two different methods: a) based on the time decay of [CO] during a street-sweeping episode, and b) based on the steady state CO_2 mixing ratio observed during time periods of known CO_2 emisions.

A) At 12:08 on 22 July 2010, the vehicles entering the tunnel were unable to pass several slow street-sweeping vehicles, leading to a large decrease in pollutant concentrations (Figure SI-S6). The 1/e decay time of [CO] is well characterized by a single exponential decay constant of 73 sec ± 2 sec, corresponding to a k_{VENT} value of 0.014 s^{-1} (used in equation 3 of manuscript text). We interpret this as a reasonable estimate of the true residence time.

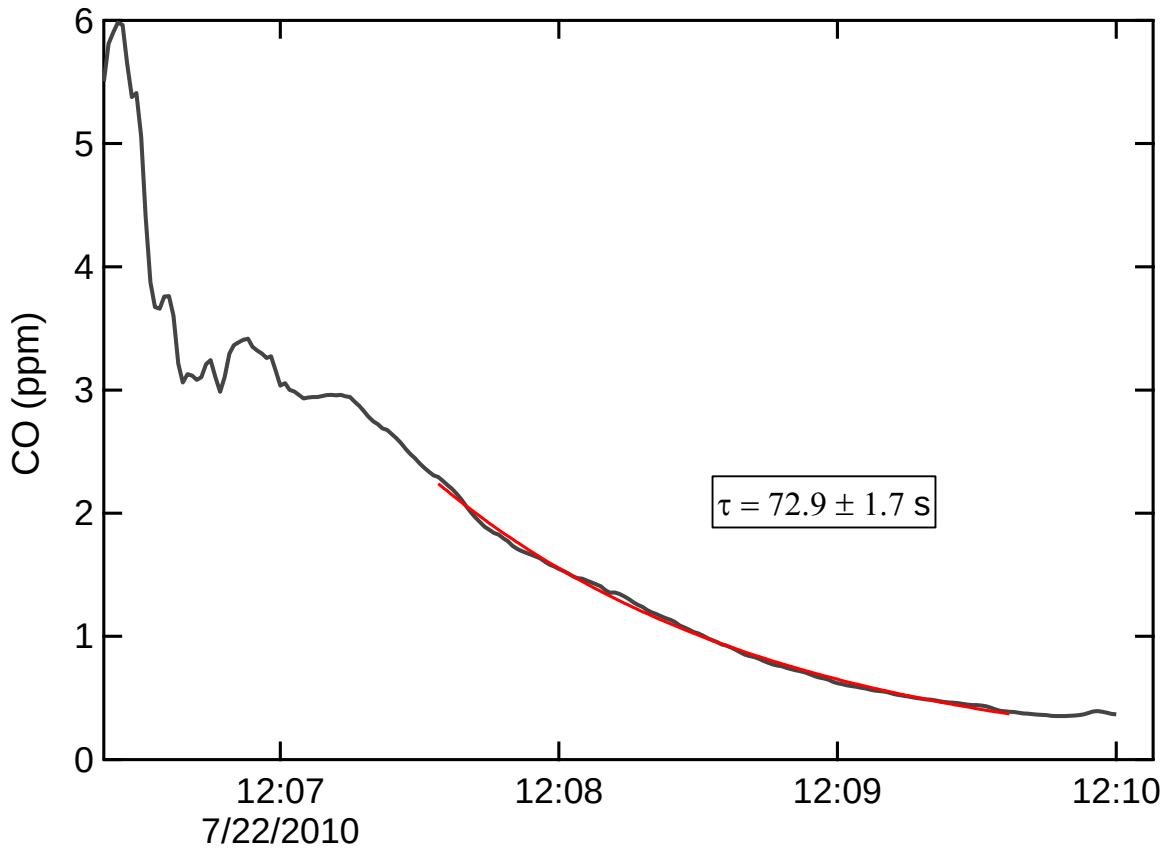

Figure SI-S5.

CO mixing ratios in the Caldecott Tunnel during the street-sweeping episode. The decay of [CO] can be fit by a single exponential with a time constant of 73 seconds, which we interpret as an upper limit to the residence time of air in the tunnel.

B) SS CO_2 method.

We infer the ventilation rate in the tunnel using a equation SI-1:

$$k_{VENT} = E_{CO2}/([CO_2]_{SS} \times V) \quad \text{(SI-1)}$$

which is the same as equation 3 in the main text. A steady state CO_2 mixing ratio of 600 ppm above the ambient background of 400 ppm corresponds to a mass concentration of 7.2×10^{-4} kg m^{-3}. The volume of the tunnel bore is 32,000 m^3. The emission rate of CO_2 (ECO_2) is calculated based on the measured traffic rates and estimates of CO_2 emission rates from vehicles.

The measured daytime traffic rate entering bore 1 of the Caldecott Tunnel was typically 2000 vehicles/hr at an average speed of 65 km/hr. Thus on average there were 31 vehicles in the 1 km long bore 1 of the tunnel. If the average fuel efficiency was 7.2 km/L (17 miles/gallon, [1]), then at 65 km/hr the average fuel consumption rate was 9.0 L/hr per vehicle. This corresponds to a CO_2 emission rate of 21.1 kg CO_2 / (hr × vehicle), assuming a fuel density of 0.76 kg/L, a fuel carbon content of 0.84, and quantitative conversion of fuel carbon to CO_2. Plugging into equation SI-1:

$$k_{VENT} = (31 \text{ vehicles} \times 21 \text{ kg } CO_2 / (\text{hr} \times \text{vehicle}))/(7.2 \times 10^{-4} \text{ kg } CO_2\, m^{-3} \times 32{,}000\ m^3) = 28.4\ hr^{-1}$$

or 0.0079 s^{-1}, which is within a factor of 2 of the CO-decay method.

For the EG emission rate calculations in the main text we use a value of $0.01 \pm 0.005\ s^{-1}$, which is the average of these two estimates of the ventilation rate and in rough agreement with tracer based measurements in the same bore of the tunnel in 2001[1].

7. Relative Concentrations of SOA Precursors in Tunnel air.

We compare the relative mass concentrations (i.e., $\mu g\ m^{-3}$, not ppb) of EG to total aromatic VOCs, total calculated IVOCs, and ethene in the Caldecott Tunnel between 07:00 and 18:00 on 27 July 2010 - a day in which the PTR-MS was online for all but 30 minutes (figure SI-S6). Aromatic VOCs and IVOCs are two classes of vehicular emissions that contribute greatly to SOA formation [3-4] via "traditional" gas-particle partitioning. The broad scope of the GC-FID/MS measurements provides excellent context to evaluate the relative importance of EG emissions in the Caldecott Tunnel. In Figure SI-S6, "AVOCs" comprises 63 individual speciated aromatic compounds listed in table 1 of Gentner et al. [2]. Select IVOCs were measured directly in the tunnel [2-3]; total IVOCs were calculated using the source contributions from the chemical mass balance (CMB) model described in Gentner et al. [3]:

$$\text{Total IVOCs} = 40.9\ \text{mol}\ m^{-3} \times 12.01\ \text{g}\ \text{mol}^{-1} \times 0.001 \times \{(D \times F_{ID}/C_{FD}) + (G \times F_{IG}/C_{FG})\}$$

where

D = ppbC of diesel exhaust,

F_{ID} = IVOC mass fraction of diesel exhaust,

C_{FD} = carbon fraction of diesel,

G = ppbC of gasoline exhaust,

F_{IG} = IVOC mass fraction of gasoline exhaust, and

C_{FD} = carbon fraction of gasoline

Ethene is included because its gas-phase oxidation by OH in the presence of NO produces glycolaldehyde with a yield of 28% [5] and thus can contribute to SOA via aqueous photochemistry.

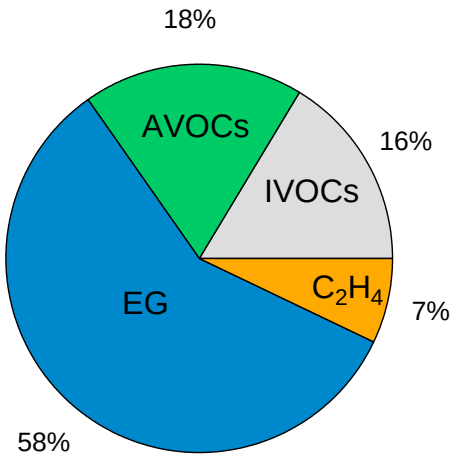

Figure SI-S6.

Relative mass concentrations of m/z 45 (mostly ethylene glycol), the sum of aromatic VOCs, the calculated sum of IVOCs, and ethene on 27 July 2010 in the Caldecott Tunnel.

EG, aromatic VOCs, IVOCs, and ethene accounted for 58%, 18%, 16%, and 7% of the total mass of these four pollutant categories on this day, respectively. On other days EG accounted for 38% to 90% of the total mass of SOA precursors. Excluding the large m/z 45 plumes over 50 ppb reduces the relative importance of EG by only 65%. Quantifying the relative importance of EG as an SOA precursor from emissions in the Caldecott Tunnel is difficult given the differences in the SOA-forming mechanisms of these compounds. SOA yields from "traditional" gas-particle partitioning are dynamic quantities that depend on ambient temperature and the mass loadings of the atmospheric absorbing phase (i.e., organic aerosol concentrations). These yields range from 4% to 10% for C6 – C10 aromatics and can exceed 100% for high carbon-number IVOCs at typical urban conditions (i.e., high-NO_x, [OA] = ~10 μg m^{-3}) [3]. The effective SOA yield resulting from aqueous oxidation depends on the extent of uptake into the atmospheric aqueous phase, the amount of oxidation, and the lifetime of the water droplet or wet particle [6]. Several VOCs (e.g., toluene) can form SOA from both gas-particle partitioning and aqueous oxidation. Additional parameters that would need to be quantified to compare SOA formation from these compounds include OH rate constants and OH concentrations, both in the gas and aqueous phases. Notwithstanding these uncertainties, the high relative mass concentration of EG does indicate the potential for it to be competitive with traditional SOA precursors from vehicle emissions from this bore of the Caldecott tunnel.

Partitioning of EG to the particulate phase would lead to increases in the SP-AMS measurements of total organic aerosol, m/z 62 or m/z 31 (following fragmentation after electron impact ionization). No increases were observed in any of these three species during the high m/z 45 events, indicating that EG did not significantly partition to the particulate phase at the existing organic

aerosol particle concentrations in the tunnel. This is not surprising given its vapor pressure ($P^*_{(25°C)}$ = 0.08 Torr): using the gas-particle partitioning equilibrium constant equation of Pankow [7-8], we calculate a C* value of 3.3×10^5 μg m^{-3}. For typical organic aerosol concentrations observed in the tunnel (40 μg m^{-3} [9]), the fraction of EG in the condensed phase would only be 10^{-4}.

179 References

180

181 1. Kean, A. J.; Harley, R. A.; Kendall, G. R., Effects of Vehicle Speed and Engine Load on
182 Motor Vehicle Emissions. *Environ Sci Technol* **2003,** *37* (17), 3739 - 3746
183 2. Gentner, D. R.; Worton, D. R.; Isaacman, G.; Davis, L.; Dallmann, T. R.; Wood, E. C.;
184 Herndon, S. C.; Goldstein, A. H.; Harley, R. A., Chemically speciated emissions of gas-phase
185 organic carbon from motor vehicles and their potential impacts on ozone and air quality. *Environ*
186 *Sci Technol* **2013,** *doi 10.1021/es401470e*,
187 3. Gentner, D. R.; Isaacman, G.; Worton, D. R.; Chan, A. W. H.; Dallmann, T. R.; Davis, L.;
188 Liu, S.; Day, D. A.; Russell, L. M.; Wilson, K. R.; Weber, R.; Guha, A.; Harley, R. A.; Goldstein,
189 A. H., Elucidating secondary organic aerosol from diesel and gasoline vehicles through detailed
190 characterization of organic carbon emissions. *Proceedings of the National Academy of Science*
191 **2012,** *109* (45), 18318-18323
192 4. Presto, A. A.; Miracolo, M. A.; Kroll, J. H.; Worsnop, D. R.; Robinson, A. L.; Donahue, N.
193 M., Intermediate-Volatility Organic Compounds: A Potential Source of Ambient Oxidized
194 Organic Aerosol. *Environ Sci Technol* **2009,** *43*, 4744-4749
195 5. Atkinson, R. J., *Gas-Phase Tropospheric Chemistry of Organic Compounds*. Natl. Inst.
196 of Stand. and Technol.: Washington, D. C., 1997; p 216.
197 6. Liu, J.; Horowitz, L. W.; Fan, S.; Carlton, A. G.; Levy, H., Global in-cloud production of
198 secondary organic aerosols: Implementation of a detailed chemical mechanism in the GFDL
199 atmospheric model AM3. *Journal of Geophysical Research* **2012,** *117*
200 (D15).10.1029/2012jd017838
201 7. Pankow, J. F., An absorption-model of gas–particle partitioning of organic compounds in
202 the atmosphere. *Atmospheric Environment* **1994,** *28*, 185-188

8. Pankow, J. F., An absorption-model of the gas aerosol partitioning involved in the formation of secondary organic aerosol. *Atmospheric Environment* **1994,** *28*, 189-193

9. Dallmann, T.; Onasch, T.; Kirchstetter, T.; Worton, D.; Fortner, E.; Herndon, S.; Wood, E.; Franklin, J.; Worsnop, D.; Goldstein, A.; Harley, R., Characterization of particulate matter emissions from on-road gasoline and diesel vehicles using a soot particle aerosol mass spectrometer. *Atmospheric Chemistry and Physics and Discussions* **2013,** *14*, 4007-4049